

Contents lists available at ScienceDirect

Journal of Aerosol Science

journal homepage: www.elsevier.com/locate/jaerosci





Laboratory evaluation of the Alphasense OPC-N3, and the Plantower PMS5003 and PMS6003 sensors

Kamaljeet Kaur, Kerry E. Kelly

Department of Chemical Engineering, University of Utah, SLC, 84102, USA

ARTICLE INFO

Handling Editor: Chris Hogan

Keywords:
PM10
Coarse particles
Low-cost sensor
Flow-focusing monodisperse aerosol generator
Aerodynamic particle sizer
Inter-sensor variability

ABSTRACT

Ambient levels of particulate matter (PM) are linked to numerous adverse health effects. However, fewer studies have evaluated the effects of coarse PM (larger than 2.5 µm in diameter), and ambient measurements of coarse PM are particularly sparse. Although low-cost PM sensors have been used to complement regulatory measurements of PM2.5, many of these sensors, such as the Plantower PMS5003, are ineffective in measuring coarse PM. The Alphasense OPCs have shown promise in detecting coarse PM and have been used in the field to measure PM₁₀ concentrations. These field evaluations have identified inter-sensor variability. Although field evaluation is critical for understanding sensor performance under environmentally relevant conditions, it provides limited information about sensor response characteristics, which are essential for determining the factors that may affect sensor measurements and contribute to inter-sensor variability. This study aims to understand these factors by conducting a size-selectivity study using monodisperse particles, and evaluating the effect of instrument-specific properties, like flow rate and laser strength, on the sensor-reported sizes and number counts. This study also evaluates a common low-cost sensor, the Plantower PMS5003, and a newer version, the PMS6003, for size selectivity. Monodisperse dioctyl sebacate particles of various diameters (2, 3, 5, 6, 9, and $10 \mu m$) were generated using a flow-focusing monodisperse aerosol generator, and the performance of nine different OPCs was evaluated. For all sizes tested, the nine OPC-N3s detected the particles, showed a peak near the target diameter, and exhibited some inter-sensor variability. The four PMS5003s and four PMS6003s detected all particle sizes but assigned all particles to the smallest size bin i.e., 0.35 μm-1 μm. With an aerodynamic particle sizer (APS) as a reference, the OPCs showed a positive bias for mean particle diameter and a coefficient of variance (CV) of less than 10%. For number concentration, the OPCs showed a negative bias, compared to the APS, and inter-sensor variability increased with the particle diameter. The laser wavelength of the OPC-N3s varied between 600 and 650 nm and appeared to have some effect on inter-sensor variability of the mean size. The flow rate reported by the OPC appeared to affect the inter-sensor variability in the number concentration.

1. Introduction

Particulate matter (PM) with a diameter less than $10 \mu m$, PM_{10} , is inhalable and has been linked to cardiovascular, cerebrovascular, and respiratory mortality (Liu et al., 2019; Orellano et al., 2020), lung cancer (Consonni et al., 2018), increased incidence of

E-mail address: kerry.kelly@chemeng.utah.edu (K.E. Kelly).

^{*} Corresponding author.

pneumonia (Yee et al., 2021), asthma (Zheng et al., 2015), stroke (Cai et al., 2022), and adverse birth outcomes (Jacobs et al., 2017). The World Health Organization (WHO) has set guidelines for 24-h and annual average PM_{10} concentration at $45 \mu g/m^3$ and $15 \mu g/m^3$, respectively (WHO, 2021). PM_{10} concentrations exceeding these guidelines have been observed during dust events, and in subway stations, schools, construction sites, and occupational settings (Araújo et al., 2014; Azarmi et al., 2016; Gomes et al., 2022; Kim et al., 2008; Lee & Chang, 2000; Singh et al., 2022; Xiang et al., 2015). PM_{10} settles quickly and tends to be more spatially heterogeneous than $PM_{2.5}$ (PM with a diameter less than 2.5 μ m) (Keet et al., 2018). However, regulatory measurements of PM_{10} are spatially and temporally sparser than $PM_{2.5}$ measurements. For example, the US EPA has 1097 active sites that measure $PM_{2.5}$ concentration but only 599 active sites that measure PM_{10} concentration (EPA, 2022).

Low-cost sensors can complement regulatory measurements to provide higher spatial and temporal resolution estimates of PM concentration in both indoor and outdoor settings (Bi et al., 2020; Caplin et al., 2019; Caubel et al., 2019; Chatzidiakou et al., 2020; Crawford et al., 2021; Do et al., 2021; Hegde et al., 2020; Li et al., 2018; Lim et al., 2019). The most commonly used low-cost PM sensors employ a laser or LED source and photodiode and estimate the particle concentrations using proprietary algorithms that convert light scattered into particle concentrations (e.g., Plantower PMS series, Honeywell HMS series, Sensirion SPS, Sharp GP2Y, etc.)(Bulot et al., 2020; Kuula et al., 2020; Sayahi et al., 2019). These low-cost sensors are generally effective for PM_{2.5}, although they require appropriate calibrations (Giordano et al., 2021). The Plantower PMS5003 is a common low-cost PM sensor that is being used in several air-quality sensor networks (i.e., PurpleAir, Clarity) and in numerous studies aimed at understanding geospatial differences in PM_{2.5} concentration and estimating PM_{2.5} exposure (Bi et al., 2020; Kelly et al., 2021; Liang et al., 2021). The PMS5003 has been evaluated extensively in the laboratory and the field, and the measurements tend to correlate well with PM₁ or PM_{2.5} concentration but perform poorly for coarse PM (particle diameter >2.5 μ m), such as PM₁₀ (Chojer et al., 2022; Kosmopoulos et al., 2020; Kuula et al., 2020; Mei et al., 2020; Sayahi et al., 2019; Singer & Delp, 2018; Vogt et al., 2021). The reasons behind this poor performance for coarse PM include the PMS's use of a polarized laser, the angular truncation of the scattered light, and particle losses (i.e., due to aspiration and impaction on the internal surfaces of the sensor)(Ouimette et al., 2022).

The Plantower PMS6003 is a newer product that utilizes two lasers for an extended lifespan of the sensor (PlanTower, 2022). The PMS6003's configuration differs from that of the PMS5003 (Fig. 1), and this sensor can be found in the PurpleAir–II–Flex sensor. The PMS6003 is also incorporated in the Clarity Node-S and is advertised to measure PM_{10} . Very limited studies have evaluated the PMS6003 performance (Demanega et al., 2021).

The Alphasense OPC-N3 is a low-cost PM sensor that shows promise for measuring particle diameters larger than PM_{2.5}. Unlike the typical low-cost sensors, which use a light source and a photodetector, the OPC-N3 also includes an elliptical mirror to capture the scattered light from a broad range of angles and a dual-element photodetector, and it allows particle counting in 24-size bins in the range of 0.35-40 µm (Technical Specifications OPC-N3 Particle Monitor, 2019). The working principle of the OPC-N3 is similar to an aerosol spectrometer, as it measures single-particle light scattering (Vogt et al., 2021). The OPCs rely on Mie theory to determine particle size, where the scattering intensity of light depends on the size, refractive index, laser wavelength, and scattering angle. The OPC-N3 comes calibrated by the manufacturer using the polystyrene latex particles (diameters ranging from 0.8 to 5 μm), and the default setting (refractive index and density) is set to that of PSL properties. Since ambient particles have varying properties, field calibrations under relevant environmental conditions are typically recommended (Barkjohn et al., 2021; Giordano et al., 2021). Several studies have found that the OPC-N3 (OPC-N3 and OPC-N2) correlate well with PM10 concentrations measured by research-grade instruments in laboratory studies (R² = 0.93–0.99) but moderately well in field studies (R²: 0.53–0.80) (Bflek et al., 2021; Crilley et al., 2018; Dubey, Patra, Joshi, Blankenberg, Kolluru, et al., 2022; Dubey, Patra, Joshi, Blankenberg, & Nazneen, 2022; Samad et al., 2021; Sousan et al., 2016, 2021). Field studies of the OPC-N2 and -N3 have reported some inter-sensor variability. Crilley et al. (2018) reported a coefficient of variance (CV) of $22 \pm 13\%$ for 14 OPC-N2 sensors for ambient PM₁₀ mass concentrations. Dubey, Patra, Joshi, Blankenberg, Kolluru, et al. (2022) did report a lower CV of 2.54–2.73% for PM₁₀ for the OPC-N2, as compared to GRIMM portable aerosol spectrometer, but they only used two sensors. Although field evaluation is critical for understanding sensor performance under environmentally relevant conditions, it provides limited information about sensor response characteristics, which are essential for determining the factors that may affect sensor measurements and contribute to inter-sensor variability.

Previous laboratory-based evaluations of the Alphasense OPC either used polydisperse particles, like Arizona Road Dust, sea salt,

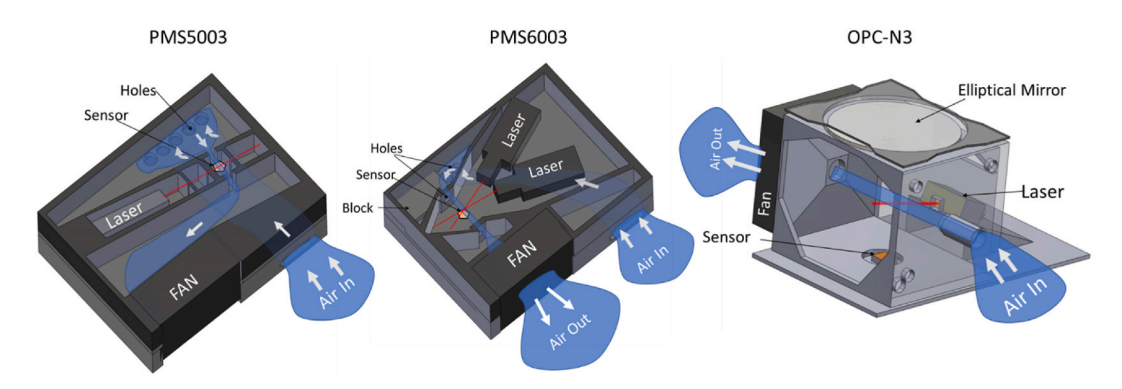


Fig. 1. Flow configuration for the PMS5003, PMS6003, and OPC-N3 sensors. Images not to scale.

welding fumes, and synthetic dust, or used monodisperse polystyrene latex beads (PSL) of diameter ranging $0.8-5 \mu m$ (Li et al., 2020; Samad et al., 2021; Sousan et al., 2016, 2021; Streuber et al., 2022). To the best of our knowledge, only one study used a large range of PSL monodisperse particles (2.5, 5.1, 7.2, and $10 \mu m$) for OPC-N2 evaluation, but it only compared the performance of two OPC-N2s with another scattering-based research grade instrument, i.e., the GRIMM portable aerosol spectrometer (PAS) 1.109 (Bezantakos et al., 2018).

This study evaluated nine OPC-N3 sensors to understand factors that may affect inter-sensor variability. It also evaluated the OPC-N3, and the Plantower PMS5003 and PMS6003 sensors for size selectivity. This study utilized a flow-focusing monodisperse aerosol (FMAG) generator, which generates highly monodisperse particles at a consistent concentration, and used the TSI Aerodynamic Particle Sizer (APS), which relies on the particle inertia to measure particle size and concentration.

2. Methods

2.1. Sensors and reference monitor

The low-cost sensors tested in this study include the Alphasense optical particle counter (OPC-N3, Alphasense Ltd, \$500), the Plantower PMS5003 (\$20) integrated into the PurpleAir II (~\$259), and the Plantower PMS6003 (\$20) integrated into the PurpleAir II Flex (\$299). Prices of low-cost PM sensors vary widely, and for this study, we define a low-cost sensor as having a purchase price of less than \$2500 (Clements et al., 2018; EPA, 2014; Giordano et al., 2021; Karagulian et al., 2019; Khreis et al., 2022). It is worth noting that if the OPC-N3 were integrated into an internet-enabled device, like the PurpleAirs, it would likely cost \$2000 - \$3000.

The Alphasense OPC-N3 uses a class 1 laser (\sim 658 nm) to detect, size, and count particles in the range of 0.35–40 μ m in 24 bins. It estimates PM₁, PM_{2.5}, and PM₁₀ concentrations from the counts using an embedded algorithm. The OPC-N3 contains an elliptical mirror to help focus scattered light from a broad range of angles onto its photodiode (Fig. 1). The default setting for refractive index (real part of 1.5) and density (1.65 g/cm³) were used in this study because these settings can only be changed by the manufacturer. The OPC-N3 uses an internal fan to create flow, and as per manufacturer, the typical sample flow rate of the sensor, is 0.28 LPM. Each OPC-N3 was connected to a laptop with manufacturer-provided software, and it stored measurements every 5 s. The measurements included the date, size bin and counts, sample flow rate, laser wavelength, relative humidity, temperature, and PM₁, PM_{2.5}, and PM₁₀ concentrations. Nine OPC-N3s were evaluated in the study, five (OPC1, OPC2, OPC3, OPC4, and OPC5) of them were purchased in April of 2021, and the remaining four were purchased in January of 2022 (OPC 6, OPC7, OPC8, and OPC9). Before this study, OPC1 - OPC5 were deployed in the field for four months, and OPC6 and 7 were each field deployed for two months. OPC1 was also used in a two-month laboratory study with incense particles. OPC 8 and OPC 9 were new.

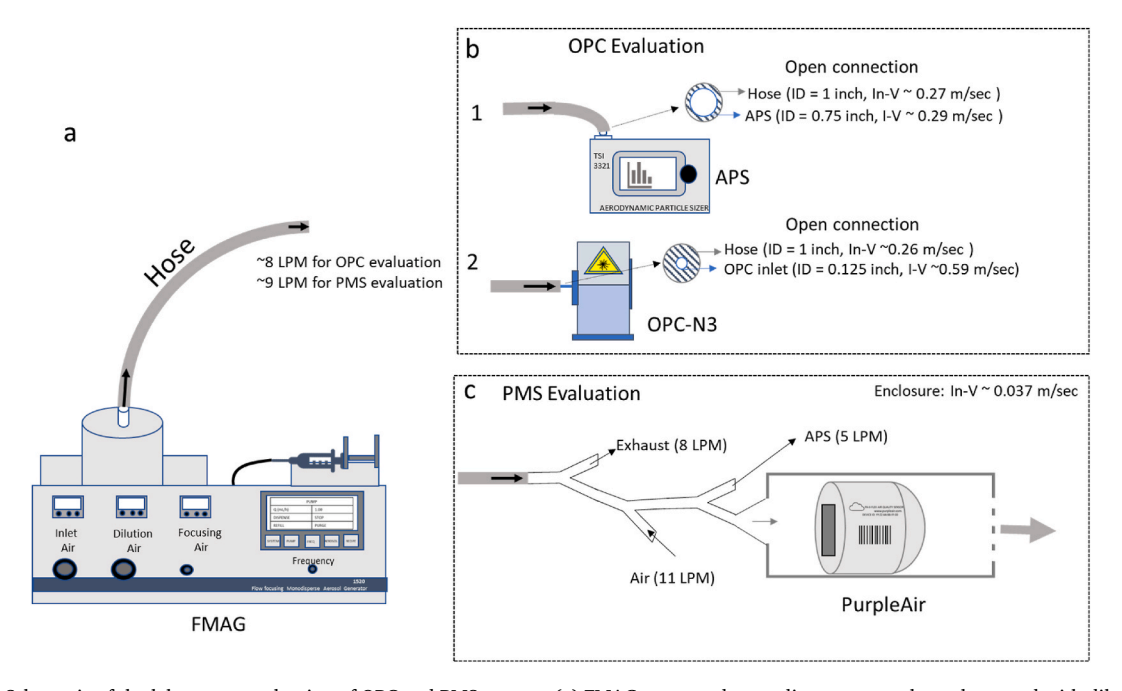


Fig. 2. Schematic of the laboratory evaluation of OPC and PMS sensors. (a) FMAG-generated monodisperse aerosol supplemented with dilution air (8 LPM and 9 LPM for OPC and PMS evaluation, respectively) (b) OPC evaluation: the FMAG-generated particles were first measured by the APS (b.1) and then by OPC-N3 (b.2). The connections between the hose (FMAG exit) and APS and OPC-N3 allowed the excess flow to exhaust to the hood. (c) PMS sensor evaluation: approximately 1 LPM flow from FMAG was diluted with particle-free air before being analyzed by the APS and PMS sensors simultaneously. The connections for the PMS evaluation were closed connections. An image of the PMS setup can be found in the supplementary material (Fig. S1). ID: inner diameter; In-V: incoming velocity; I-V: inlet velocity.

This study also evaluated the Plantower PMS 5003 and PMS6003 low-cost sensors, integrated into the PurpleAir II and the PurpleAir-PAII-Flex, respectively. PMS sensors are quasi-nephelometers, which use a fan to create flow (\sim 0.1 LPM), a red laser (\sim 680 \pm 10 nm), a scattering angle of 90°, and a photo-diode detector to measure total scattering from a plume of particles. The PMS sensor converts the total light scattering into several different air quality parameters, including particle counts (0.3–10 μ m), PM1, PM2.5, and PM10 using an embedded algorithm. Unlike the PMS5003, the PMS6003 deploys two lasers for increased sensor lifespan (PlanTower, 2022). Fig. 1 shows the flow configuration of the two PMS sensors. For both sensors, the flow path involves more than one 90-degree turn before reaching the photodiode. The PMS6003 includes a feature to avoid possible stagnation and sharp corners ('Block' in Fig. 1). The particle counts, PM1, PM2.5, and PM10 measurements with a collection frequency of 2 min were downloaded from the PurpleAir database or stored in the SD card. This study used the particle counts for the different bins without any additional corrections. Two Purple Air II (named PA1 and PA2) and two PurpleAirPA-II Flex (named Flex 1 and Flex 2), each containing two sensor nodes, were evaluated in this study. Before this study, PurpleAir II and PurpleAir-PAII-Flex were field deployed for two months.

This study used the aerodynamic particle sizer (APS, TSI 3321, TSI Inc., Minneapolis, USA) as a reference. The APS measures the aerodynamic size (diameter) of particles in the range of $0.523 \, \mu m$ – $19.81 \, \mu m$ in 52 size bins. Each scan of APS required 20 s. APS data were recorded using manufacturer-provided software AIM 8.1.0.0.

2.2. Study design

This study aims to evaluate the size selectivity of OPC-N3, PMS5003, and PMS6003, and instrument factors in the OPC-N3 that may affect inter-sensor variability. The sensors' performance was evaluated with monodisperse aerosols generated using the FMAG (discussed in the next section). Monodisperse particles with diameters of 2, 3, 5, 6, 9, and 10 μ m were used for the evaluation of OPC-N3, and diameters of 2, 5, and 10 μ m were used for the PMS sensors.

2.2.1. Evaluation of OPC-N3

Because the OPC-N3 allows measurement of high number concentrations (10,000 particles/sec) the flow leaving the FMAG (8 LPM of dilution air) was not diluted further. The FMAG-generated monodisperse particles flowed through a 1–inch hose (inner diameter, provided by the FMAG manufacturer, Fig. 2a) to the APS (Fig. 2b.1). The connection of the APS and FMAG outlet (the hose) was not closed (Fig. 2b.1), i.e., the APS inlet of ¾ inch was loosely connected to the 1-inch hose (FMAG exit) such that excess flow escaped into the hood. The suction velocity of APS (0.29 m/s) was also slightly greater than the incoming velocity from the hose (0.26 m/s). The APS confirmed the particle size distribution (PSD) of the FMAG-generated aerosols. A minimum of ten, 20-s APS measurements were collected to ensure the stability of the FMAG's PSD. Later, each OPC-N3 sensor was evaluated individually. For the OPC-N3, its inlet (inner diameter of 1/8 inch) was adjusted to be in the center of the FMAG's outlet hose. The connection was open (Fig. 2b.2), i.e., the excess flow escaped into the hood. The inlet velocity of the OPC-N3, using the manufacturer-provided flow rate of 0.28 LPM, was 0.59 m/s, which exceeds the velocity in the FMAG's exhaust (1-inch hose with a velocity of 0.26 m/s). Each OPC-N3 collected measurements for 5 min with a sampling interval of 5 s. The measurements from the OPC-N3 were stored on a laptop using the manufacturer-provided software. At the end of the evaluation of all OPC-N3s for each target diameter, a minimum of three APS measurements were collected (three 20 s runs) to ensure that the PSD did not shift during the testing. To check the reproducibility of the OPC-N3 sensor response, four of these sensors were evaluated a second time for the 2, 5, and 10 µm target diameters.

2.2.2. Evaluation of PMS sensor

Due to the PMS sensor's limit on PM mass concentration (maximum range $<1000 \,\mu\text{g/m}^3$ for PM_{2.5}), the flow exiting the FMAG was diluted. The flow exiting the FMAG was divided using Y connectors (inner diameter of 1 inch). One end of the first Y connector was connected to a pump that drew a set amount (8 LPM), and the remaining was diluted with particle-free air (11 LPM, controlled using a mass flow controller) using another Y connector (inner diameter of 1 inch) (Fig. 2c). The diluted flow was further divided using a second Y connector, with one end connected to the APS (taking 5 LPM), while the other end was connected to the enclosure (dimensions 8x4x4 inches) with an inlet in the form of a funnel (Fig. 2c). The diameter of the funnel end connected to the enclosure was \sim 2.5 inches. The PMS sensors were placed in the enclosure, with the inlet facing the incoming aerosol (to assist with aspirating the coarser PM), and sampled for a minimum of 20 min with a 2-min sampling interval. The incoming velocity of the monodisperse particles into the enclosures was approximately 0.037 m/s, which is lower than the typical ambient wind speed (1–3 m/s) (Ouimette et al., 2022). The PMS measurements were stored in the PurpleAir cloud for the PMS 5003 and stored on an SD card for PMS 6003. Unlike the OPC-N3s, continuous APS measurements were taken while evaluating the PMS sensors.

2.3. Monodisperse particle generator

This study used monodisperse particles generated using FMAG (FMAG 1520, TSI INC., USA). The details of FMAG can be found by Duan et al. (2016). Briefly, the FMAG squeezes a liquid (a mixture of a non-volatile solute and solvent) through a nozzle to form a jet using coaxial flow-focusing air. This jet is disrupted by mechanical vibrations to create droplets of uniform and target diameter (more information on the working theory in supplementary material). The droplets can then be dried using particle-free air to obtain particles (solid or liquid) of a known diameter. The FMAG can be used to calibrate other PSD measuring instruments, like the APS or GRIMM. According to the manufacturer, the FMAG can generate particles with a diameter ranging between 0.8 μ m-8.5 μ m (solid) or 0.85 μ m-12 μ m (liquid) with a geometric standard deviation of <1.05 for liquid/solid particles (TSI, 2022).

In this study liquid particles with target diameters of 2, 3, 5, 6, 9, and 10 µm were generated using the FMAG. Dioctyl sebacate

(DOS, Sigma Aldrich, density of 0.914 g/cm³) was mixed in a known volumetric concentration of isopropyl alcohol (IPA, 99.99%, Sigma Aldrich). The FMAG-generated liquid particles are spherical (Duan et al., 2016) and are a good candidate to explore the size selectivity of the OPC-N3 and PMS sensors, as they assume the particles to be spherical. The concentration of DOS, vibration frequency, and injection flow rate were adjusted to obtain the target diameter (Table 1). For the OPC-N3 evaluation, the dilution air flowed at a rate of 8 LPM and was used to dry and transport the particles. For the PMS sensor evaluation, the dilution flow rate was 9 LPM. The flow-focusing pressure (ΔP) was fine-tuned to narrow the PSD peak (Table 1).

The minimum target diameter used in the study was $2 \mu m$. The target diameter of $1 \mu m$ was attempted, but the background from the IPA was substantial, producing bimodal instead of a single mode of monodisperse particles. Consequently, this study evaluated the size selectivity of OPCs and two different PMS models at sizes of $2 \mu m$ and larger.

For the blank/background measurements, the syringe pump was not operated (not producing any particles) and the rest of the system was operated as normal. All the sensors and APS returned zero counts (data not included) for the blank measurements.

3. Data analysis

For aerodynamic particles bigger than 4 μ m, the APS-reported aerodynamic diameters were first corrected for size shift caused by the deformation of the liquid droplets (Chen et al., 1990; Duan et al., 2016) and the nozzle constriction using correction equations provided by Baron et al. (2008) for DOS particles:

$$d_{a_m} = d_a + \Delta$$

With $d_{a,m}$ as the aerodynamic diameter provided by the APS, d_a as the corrected aerodynamic diameter, and Δ is the size shift in micrometers, taken from Baron et al. (2008):

$$\Delta = -a * d_a^b / (\eta^c \sigma^e)$$

With η as liquid particle viscosity in Pa-s (0.027 Pa-s for DOS) and σ as the liquid surface tension in N/m (0.0322 N/m for DOS). The a, b, c, and e were the fitted constant for APS model 3321 and were 2.723*10⁻⁴, 2, 0.6486, and 0.3864, respectively (Baron et al., 2008). The APS bins starting with a mean bin size of 4.05 μ m were corrected. The detailed bin sizes are shown in the supplementary material (Table S1).

The OPCs report particle diameter based on light scattering, which is equivalent to particle geometric diameter for spherical particles. The FMAG liquid-generated particles are reported to be spherical. For a better comparison between the low-cost sensors and APS, the corrected APS aerodynamic diameter D_a was converted to particle geometric diameter using the correlation below (Duan et al., 2016):

$$D_p = \left(\frac{\rho_o}{\rho_p}\right)^{0.5} D_a$$

Where, D_p the particle diameter (geometric), ρ_o is the density of the water (taken as 1 g/cm³), ρ_p is the density of the particle (taken as 0.914 g/cm³ for DOS), D_a is the corrected aerodynamic diameter of the particle. All the further data analysis was performed using D_p .

The particle number concentrations provided by the APS were corrected for the counting efficiency by dividing the APS-reported number concentrations by the counting efficiency. Similar to the work described by Volckens and Peters (2005) and Tryner et al. (2020), the APS's counting efficiency for liquid particles of diameter 0.8 μ m is approximately 0.75 and this efficiency decreases linearly to 0.25 for a particle diameter of 10 μ m. The efficiency for particles smaller than 0.8 μ m and bigger than 10 μ m was assumed to be constant at 0.75 and 0.25, respectively. Although the particles were primarily monodisperse, there was a size distribution, resulting in some particles smaller than 2 μ m and some larger than 10 μ m, depending on the target diameter. The corrected total number concentration, including any noise peak, was used to assess the bias in the number concentrations reported by OPC-N3.

For the updated APS size bins, i.e., in terms of D_p and the corrected number concentrations, the mean, mode, median, total number concentration, and geometric standard deviation for each measurement were calculated using the equations provided by the manufacturer in the APS manual (TSI, 2006). The mean D_p was used to evaluate the bias in the mean diameter reported by OPC-N3, for all the target diameters tested.

Table 1 FMAG conditions used to generate monodisperse particles.

Target diameter (μm)	DOS Conc in IPA (V/V)	Frequency ΔP (psi) (kHz)		Q Injection Flow rate (mL/hr)	Theoretical Geometric Particle diameter (μm)		
1	1.25E-4	120	1.04	2	1.03		
2	1.25E-4	62.1	0.91	7.5	2.00		
3	1E-3	69	0.61	3.5	3.00		
5	2.5E-3	69	0.87	6.5	5.00		
6	1E-2	67.5	0.61	2.85	6.07		
9	2E-2	64	0.60	4.6	9.14		
10	2E-2	79.3	1.01	7.5	10.0		

 D_p based APS bins were used for plotting the PSD. To compare the PSDs between the APS and the OPC-N3, the number concentrations (#/cm³) were converted to dN/dlogD_p The details of the APS bin lower bounds, upper bounds, and bin width in terms of D_p can be found in Table S1 (Supplementary material). To compare the APS measurements with the PMS PSD, the APS bins were grouped into five bins: 0.3–1 µm, 1–2.5 µm, 2.5–5 µm, 5–10 µm, and >10 µm, based on the geometric diameter (D_p). To do so, for every APS measurement, the particle counts were summed to the corresponding size bin intervals. When the exact upper limit or lower limit (0.3, 1, 2.5, 5, and 10 µm) was not available in the APS bins, the nearest bin limit was used. For example, counts between APS mean bin sizes of 1.009 µm–2.57 µm were used to represent the PMS 1–2.5 µm size bin.

For the OPC-N3, the mean particle size (diameter) was measured from the number counts and mean bin diameter. The number concentrations (#/cm³) were obtained by dividing the number counts (#/sec) by the OPC's reported sample flow rate (mL/s). For the OPC-N3, bias in total number concentration and mean particle diameter was calculated using the APS as the reference. The bias was

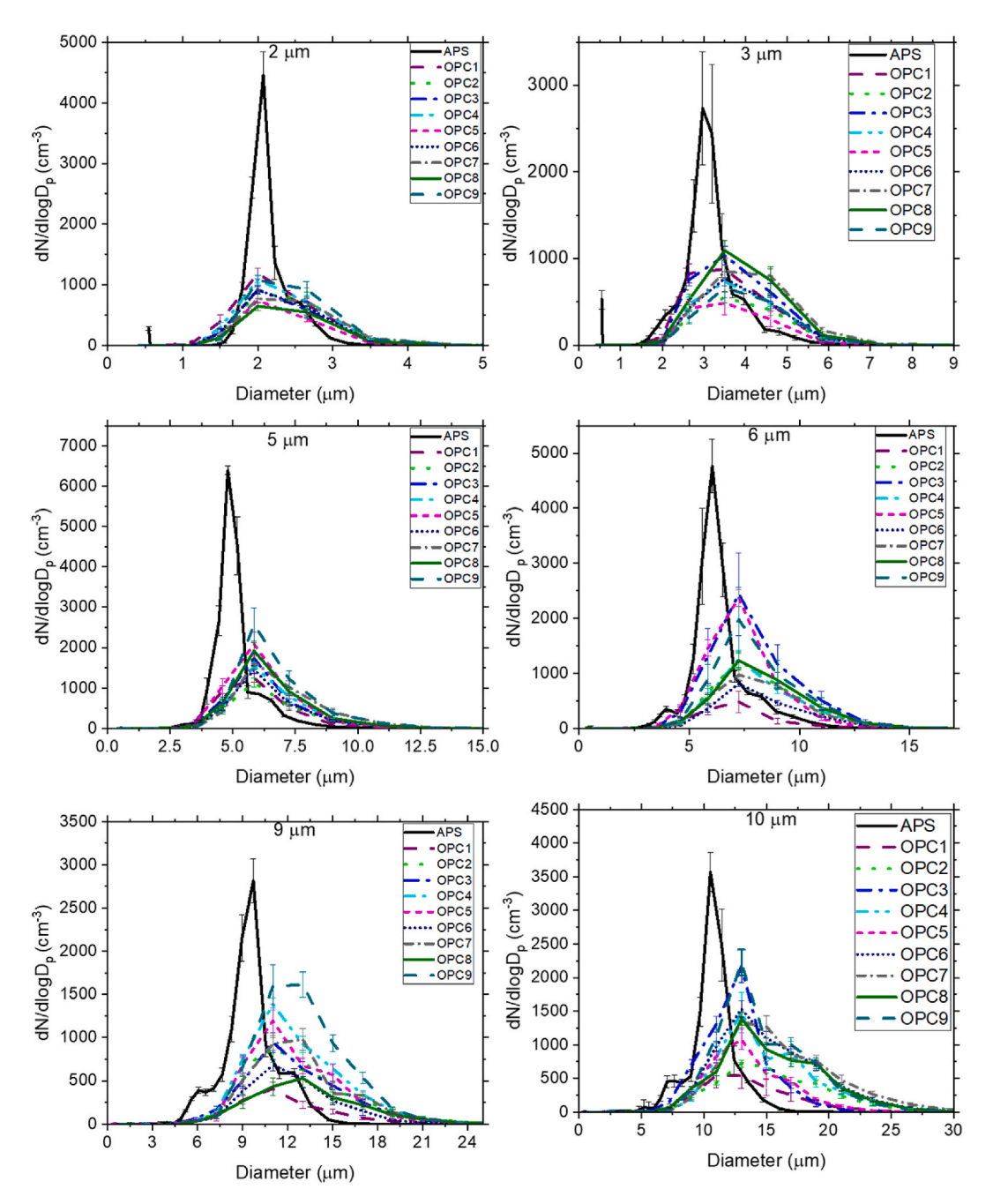


Fig. 3. PSD measured with 9 OPC-N3s and one APS for different monodisperse target diameters. Error bars represent standard deviation (n = 60 for OPC; n = 10 for APS). PSD in terms of absolute number can be found in the supplementary material (Fig. S2).

calculated using:

Bias% =
$$\frac{1}{N} \sum_{1}^{N} \frac{Y_{OPC} - Y_{APS}}{Y_{APS}} * 100$$

where N is the total number of runs, Y_{OPC} is the OPC measurement, and Y_{APS} is the APS measurement. The measurements include total number concentrations ($\#/\text{cm}^3$) and mean particle size (μ m). The effect of the OPC's measured flow rate on the number bias and the effect of the OPC's reported laser wavelength on the mean particle diameter were also evaluated.

The coefficient of variance (CV) was used to measure the precision, reproducibility, and inter-sensor variability of the OPC-N3 sensors using the following equation:

$$CV = \frac{\sigma}{m} * 100$$

Where σ is the standard deviation and m is the mean of the measurements. The OPC measurements include the total number concentration and mean particle size measures. Although low-cost sensor performance guidelines are not available for particle counts or PM₁₀ concentrations, the US EPA's performance guidelines for PM_{2.5} sensors recommends a CV value of less than 30%, and this guideline is used for discussion purposes (Duvall M. R. et al., 2021).

4. Results and discussion

4.1. FMAG

The monodisperse particles generated by the FMAG had a mean diameter close to the target diameter (Fig. 3). The mean diameter obtained from the APS (D_p) was within 5% of the target diameter. Table 2 provides the mean and CV values for the different FMAG target diameters. It indicates that the CV values primarily remained below 3% and that the FMAG produced stable particle diameters. For target diameters of 2 and 3 μ m, the APS measurements revealed a peak for the diameter <0.54 μ m, which could be due to the background from solvent and solute (Fig. 3). The particle size is considered monodisperse if the GSD is less than 1.25 (Japuntich et al., 1990). A somewhat higher GSD was observed for the 9 and 10 μ m target diameters, mostly due to the shoulder peak. A shoulder peak was observed for all target diameters, and this shoulder became more visible with increasing target particle diameter (Fig. 3). This could be due to the doublet formation, i.e., coagulation of single droplets (Duan et al., 2016). Although the fraction of doublets was minimized by tweaking the frequency, the shoulder peaks were not fully eliminated. The increasing solute background associated with increasing DOS concentration could also be another reason for the shoulders.

4.2. Performance evaluation of the OPC-N3

Fig. 3 shows the PSD obtained from the 9 different OPC-N3s for 6 different monodisperse particle diameters. For all the diameters tested, the OPC-N3 exhibited a peak near the target particle diameter, although the peaks were broader than the APS, which could be due to the larger OPC-N3 bin sizes. The OPC-measured peak magnitude (Fig. 3) is higher for the APS and is due to the smaller size bins as compared to the OPCs. Fig. 3 also shows that the peaks were shifted to the right compared to the APS. This variation was expected because the OPC-N3 was pre-calibrated by the manufacturer with polystyrene latex (PSL) particles, which have a different refractive index (1.59+0i) compared to the DOS particles (1.45 +0i). The different refractive indices may result in different bin assignments (Hagan & Kroll, 2020). Also, the OPC's large and non-uniform bin sizes further affected the reported mean sizes. For example, the bin width for the OPC-N3 increases from about 0.5 μ m at 2 μ m, to 1 μ m at 3 μ m and to 2 μ m at 8 μ m, which could also contribute to the increasing bias with the target diameter.

The nine OPC-N3s exhibited some inter-sensor variability in mean particle diameter, and the difference remained somewhat consistent irrespective of the target diameter (Fig. 4). Although the bias with respect to APS in mean diameter increases with the target diameter, the difference in the bias between sensors was generally less than 30%. The CV for the mean diameter measured by the nine OPCs varied between 3.86 and 7.47% (Table 3), well within the EPA CV guideline, for all target diameters tested. OPC1 reported the lowest mean diameter among all sensors for all target diameters tested (Fig. 4 left). OPC7 and OPC9 reported the greatest mean

Table 2

APS measurements of monodisperse particles for the different FMAG target diameters, used for evaluation of OPC-N3s. The values correspond to average values with the CV (%) in parentheses. The diameter corresponds to the particle geometric diameter (D_p), which was obtained by converting the corrected APS aerodynamic diameter to geometric diameter. The APS concentrations were corrected for counting efficiency. Table S2 shows the APS measurements collected during PMS sensor evaluation.

	2 μm	3 μm	5 μm	6 μm	9 μm	10 μm
Median (µm)	1.96 (1.77)	2.89 (3.37)	4.66 (3.97)	5.73 (3.67)	8.89 (2.53)	10.39 (4.17)
Mean (µm)	2.11 (0.72)	3.06 (2.01)	4.99 (1.11)	6.14 (1.30)	9.17 (0.96)	10.36 (2.47)
Mode (µm)	2.07 (0.00)	3.01 (2.98)	4.81 (0.00)	6.05 (0.00)	9.65 (2.08)	10.52 (0.00)
GSD	1.13 (0.37)	1.24 (1.44)	1.16 (0.15)	1.22 (1.81)	1.26 (0.68)	1.23 (3.96)
Total Concentration (#/cm ³)	437 (1.72)	514 (7.15)	656 (0.61)	564 (2.81)	376 (2.69)	406 (6.02)

diameter among all the sensors. (Fig. 4).

Several factors may be responsible for the observed inter-sensor variability. OPC-N3 relies on measured scattered intensity and other known parameters (refractive index, shape, wavelength, etc.) to infer the radius of a particle. Typically, a pre-generated calibration curve (scatter intensity vs. radius) is used to infer the radius using the measured scattered intensity. Mie's theory describes how scattered intensity by a particle depends on particle size, shape, concentration, refractive index, the wavelength of the incident light, the polarization of the incident light, scattering angle, and the angle of observation. Several of these factors (refractive index, scattering angle, observation angle, and particle shape) remained constant for all experiments and OPCs in this study. Furthermore, the particle counts in this study were well within the manufacturer's recommended range, and therefore the particle concentration was not considered as a factor in inter-sensor variability. It is also possible that deposits on the OPC's elliptical mirror and photodetector may affect inter-sensor variability, but this was not evaluated because examining deposits would require opening the OPCs and voiding the manufacturer's warranty. Consequently, this study examined laser performance as a factor in the inter-sensor variability of particle size (Fig. 5).

Fig. 5 shows that the laser wavelength of the nine sensors varied between 600 and 650 nm. The wavelengths for OPC8 (~605 nm) and OPC1 (~640 nm) were at the edges of this range for all target diameters (Fig. 5). OPC1 had the lowest wavelength and the lowest mean size. OPC8 had the highest wavelength and exhibited the highest mean size for most cases. For the sensors OPC2 -7, the wavelength varied between 617 and 629 nm, and the mean sizes varied with the target diameter but remained higher than OPC1 (highest wavelength). Overall, the OPC-reported mean particle diameters tended to decrease with increasing wavelength. This observation correlates well with the Mie theory, where for a particle diameter larger than the incident wavelength (as in this study), the scattering coefficient decreases with increasing wavelength (Purcell & Pennypacker, 1973). A decreased scattering coefficient implies decreased scattered light intensity, at a given angle, and since the OPCs estimate of size is based on the scattered intensity, a lower scattered intensity would result in sizing the particle smaller than the actual size. The variation in mean particle diameter could also be caused by dust accumulation on the OPC's elliptical mirror or any impurities in the sensor's optics that can affect scattered light and consequently the size estimated by the OPC-N3 (Bezantakos et al., 2018).

For all target diameters except for 9 μm and 10 μm (Fig. 4 right), the OPCs underestimated the number concentration compared to the APS. For the 10 μm target diameters, two of the sensors had a positive bias, whereas the remaining seven showed a negative bias. For particles greater than 10 μm , the counting efficiency of the APS was assumed to be the same as that of 10 μm , which may lead to an underestimation of the number concentration from the APS, which affected the calculated biases for the OPC-N3. The range of sensor bias also increased with target diameter, i.e., the bias ranged between -60 and -32% for 2 μm , and this range increased to -75 to 7% for 10 μm . This was also evident from the increase in CV values. The CV was 19.4% for 2 μm , and this increased to 34.2% for 10 μm (Table 3). The CV values for number concentration were mostly less than 30%, within EPA guidelines.

The OPC number concentrations were calculated using the counts/sec and the flow rate (mL/sec) provided by the software. As the target diameter increased, the variation in the particle counts also increased (Fig. S3). To elucidate the effect of the reported flow rate on inter-sensor variation in particle counts, the counts were divided by the manufacturer's reported flow rate, i.e., 4.67 mL/s to obtain number concentrations, which was used to obtain bias compared to the APS measurements (Fig. S4). From Table 3, the CV was less than 30% (5.8–21.7%) for all target diameters when using the constant flow rate although the CV was highest for the 9 μ m and 10 μ m target diameters. The concentration of the large particles may be more spatially heterogeneous and a slight difference in the sampling position could affect the counts and the corresponding number of concentrations. Mukherjee et al. (2017) noted the orientation and position of the sensor inlet is important when sampling large particles like dust.

Table 3 shows that the CV (19.5–47.1%) was higher when using the sensor-reported flow rate compared to the constant flow rate. For the nine sensors, the flow rates differed from the manufacture-specified sample flow rate of 4.67 mL/s (1–16 mL/s; x-axis on Fig. 6,

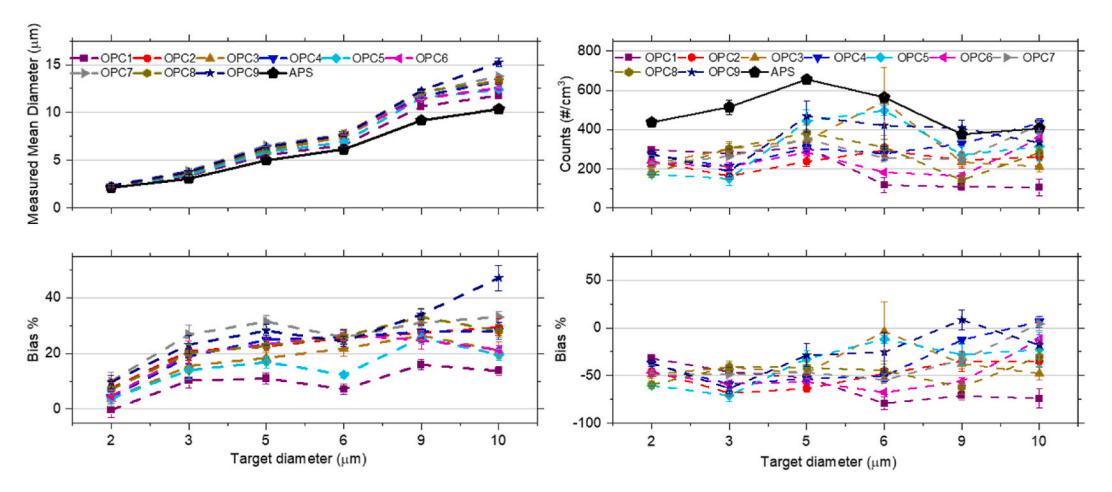


Fig. 4. (Left) Mean particle diameters measured by the OPC-N3s and their bias (compared to the APS). (Right) Total number concentrations and bias compared to the APS measurements. Error bars represent standard deviation (n = 60 for OPCs, n = 10 for APS).

Table 3CV in mean diameter and total number concentration measured by the nine OPC-N3s.

Target particle diameter (μm)	CV mean diameter (%)	CV concentration using sensor-reported flow rate (%)	CV concentration (%) assuming a constant flow rate of 4.67 mL/s $$
2	3.86	19.5	11.4
3	4.75	26.4	5.80
5	5.39	23.8	7.80
6	5.77	47.1	16.4
9	4.43	38.6	21.7
10	7.47	34.2	19.5

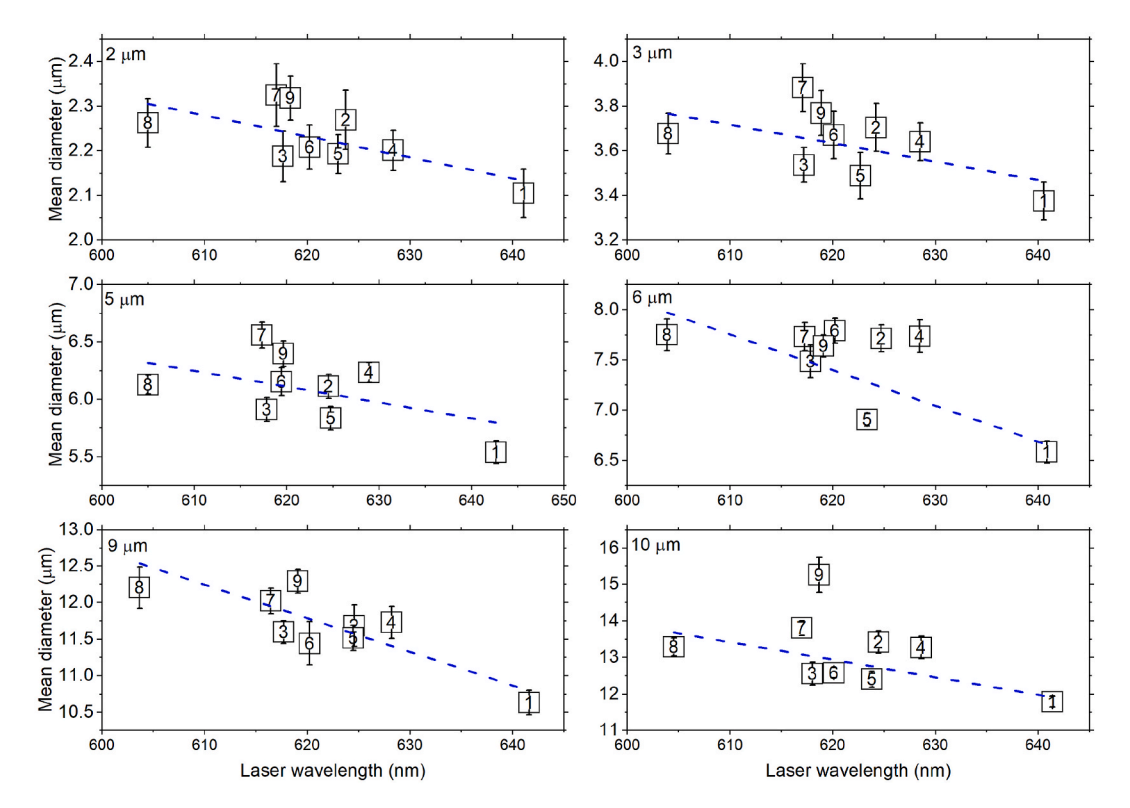


Fig. 5. Effect of laser wavelength on the mean size. Dashed lines represent the general trend in the mean size with laser wavelength. Error bars represent standard deviation (n = 60).

Fig. S5) and differed with the target diameter. For example, for target diameters of 9 μ m and 10 μ m, OPC1 flow rates were high, 15–16 mL/s, which resulted in large sensor-to-sensor variation (number bias: -75 to 7%) (Figs. 4 and 6). This indicates that the variability in the reported flow rate by the sensor affects the inter-sensor variability for particle concentrations. Because the number concentrations were determined by dividing the counts by the sensor-reported flow rates, a good correlation exists between the flow rate and the number bias (generally $R^2 > 0.78$, Fig. 6). The reason behind the variable flow between sensors is unknown. According to the manufacturer, the flow rate is determined by the time-of-flight method, but it is unclear how this time-of-flight measurement is performed within the OPC-N3. Other than the sensor placement and flow rate, factors affecting the OPC-N3's measurement of number concentration include particle aspiration efficiency, particle losses within the sensor, and optical system performance (i.e., dust on the elliptical mirror or photodetector).

Four of the OPC-N3s were tested for reproducibility to monodisperse target diameters of 2, 5, and $10 \, \mu m$. Fig. 7 shows that the bias in the mean diameter had repeatable trends and magnitudes. The CV for the two runs for the mean measured diameter remained less than 10% (Table 4). A variation in the concentration bias was observed between the two runs. The CV (number concentration) for OPC6 remains less than 10%, but the other OPC-N3s showed somewhat higher CV values (8.49–38.5%). Again, the number concentration may be affected by the sensor placement and the variable flow rates of the sensors, and the placement of the inlet. More consistent behavior between the two runs was observed if using the constant flow rate of 4.67 mL/s for estimating the number concentration for the OPC (Fig. S12).

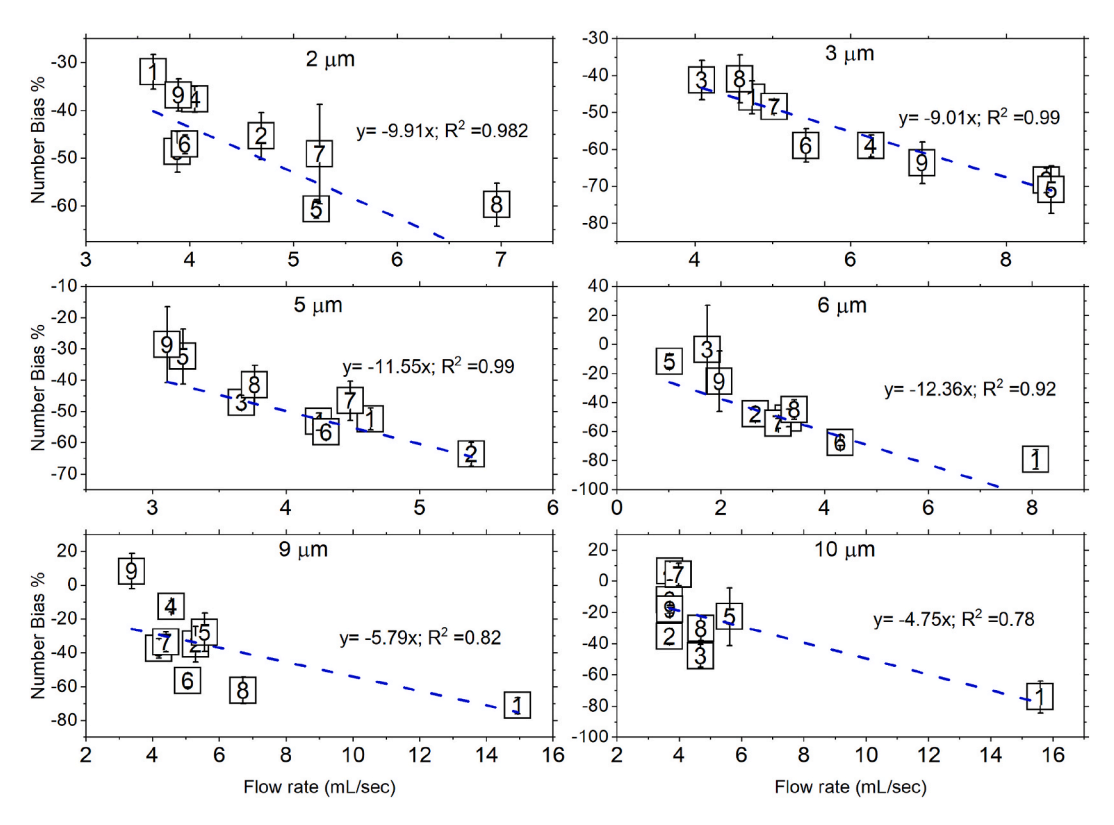


Fig. 6. Effect of the OPC-N3 flow rate on the concentration bias. Error bars represent standard deviation (n = 60).

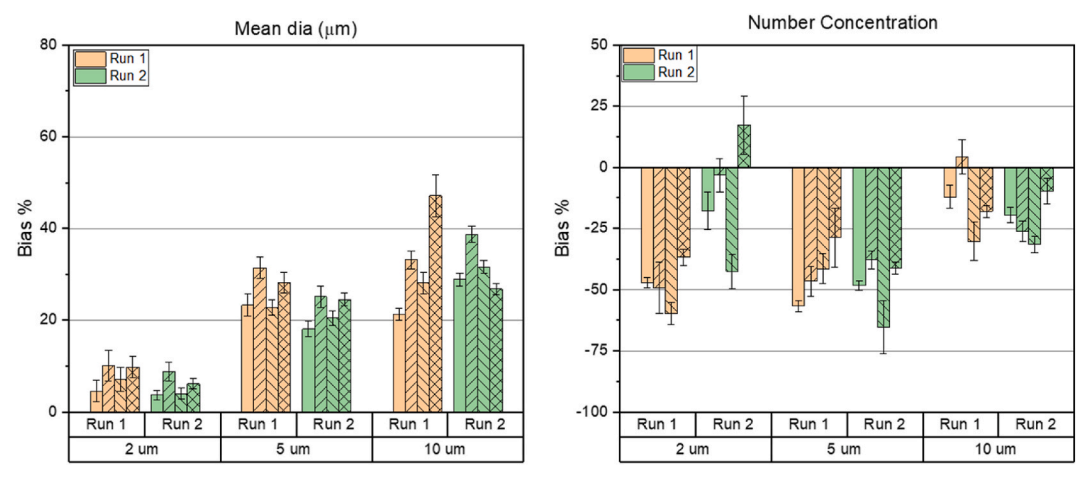


Fig. 7. Reproducibility of four of the OPC-N3s for three monodisperse target diameters (2, 5, and 10 μ m). Error bars represent standard deviation (n = 60).

Table 4CV in mean diameter and total number counts for two different runs for four of the OPC-N3s.

Target particle diameter (μm)	CV mean diameter (%)				CV concentration (%)			
	OPC6	OPC7	OPC8	OPC9	OPC6	OPC7	OPC8	OPC9
2	2.73	3.34	3.68	3.75	8.40	13.3	13.5	10.6
5	1.72	1.97	1.45	1.37	5.36	8.49	38.5	19.2
10	4.75	3.99	3.40	5.24	6.44	9.40	10.3	13.5

4.3. Performance evaluation of the PMS sensors

Both the PMS 5003 and PMS 6003 did respond to all target diameters, although they underestimated particle concentration for most cases and appeared incapable of correctly binning particle sizes (Fig. 8). This finding is consistent with the previous study by Kuula et al. (2020) and Tryner et al. (2020). Both the Flex and PA reported similar total number concentrations (sum concentration of all the bins) to the APS for the target diameter of $10 \mu m$ (Fig. S7), but the reported PM₁₀ concentration was three orders of magnitude lower than the APS reported PM₁₀ concentration (Fig. S10). The incorrect binning of the particle strongly affects the reported PM concentrations by these sensors and therefore the reported PM₁₀ concentration for large particles, like dust, is unreliable. Studies using the PMS sensor for measuring dust and coarser particles have reported little to no response by the PMS sensor (Demanega et al., 2021; Kosmopoulos et al., 2020; Sayahi et al., 2019).

The big particles are susceptible to pneumatic handling, and since more fitting and connections were used for the evaluation of the PMS sensor, variability in the APS measurements was higher as compared to that observed for the APS measurements taken during OPC evaluation.

5. Limitations

This study does have some limitations. It utilized liquid particles, which deform when accelerated inside the APS. A solid salt particle would be an alternative, but the salt-solution particles can only be generated up to a maximum diameter of approximately 8.5 μ m (TSI, 2022). Polydisperse particles like dust and salts have been utilized to calibrate the low-cost sensor for PM mass concentrations (Samad et al., 2021; Sousan et al., 2016, 2021). This study sought to systematically understand the OPC-N3, PMS5003, and PMS6003 sensor response to monodisperse particle diameters up to 10 μ m in diameter; consequently, we selected liquid particles, despite their limitations.

The age of the sensors was not considered and could be a significant factor influencing inter-sensor variability. The OPC aging, i.e., previous usage in the field studies, can result in dust depositing on the elliptical mirror, laser, fan, or photodiode, and possible corrosion of the elliptical mirror. Bezantakos et al. (2018) identified dust deposition in the OPC-N2 affected the mean diameter measurements. The accuracy of the OPC-N3 reported laser wavelength and the flow rate relied on the manufacturer-reported value and was not verified because the measurement of these factors requires opening the OPC-N3, which would void the manufacturer warranty.

The solvent and solute used in the FMAG have trace impurities that resulted in a background noise peak at the lowest bin (<0.547 μm) visible for the 2 μm and 3 μm target particles. This study included the peaks in the total number concentration. Previous studies working with the PSL particles ignored the background noise peak at the lowest bin size for the GRIMM 1.109 (Bezantakos et al., 2018). This study did not ignore these peaks because the smallest bin of APS, i.e., 0.54 μm (in terms of geometric diameter) is larger than the OPC's smallest bin (i.e., 0.35 μm). Including the background, noise peak would affect the calculation of bias in this study, but it would not affect the trends in bias associated with number concentration.

Unlike the APS, the PMS sensor uses a small fan to pull the required flow, and its inlet has several circular holes. As no closed connection was possible for the PMS sensor, the sensors were placed inside an enclosure, this resulted in different modes of connection between the APS and PMS sensor. In addition, the connection from the Y-fitting to APS was conductive tubing that included a 180° bend in form of an arc (Fig. S1). This could cause losses for larger diameter particles, and therefore an underestimation of the APS's number concentration. The difference in mode and tubing-associated losses could result in additional bias in the number concentration of the PMS sensor relative to the APS but would not affect the size of the particles. In general, larger particles ($>5 \mu m$) are susceptible to differences in pneumatic handling and are more heterogeneous than smaller particles. Consequently, the higher variability in sensor measurements for the larger particles could due to the sensor's connection or placement.

6. Conclusion

This study evaluated the performance of the Alphasense OPC-N3, PMS 5003 (PA), and PMS6003 (Flex) sensors in response to monodisperse DOS particles ranging in diameter from 2 to 10 μ m. For all target diameters tested, the OPC-N3s detected the particles and showed a peak near the target diameter. The PMS5003 and PMS6003 did appear to detect the particles but assigned all particle sizes to the smallest size bin i.e., 0.35 μ m-1 μ m. With the APS as a reference, the OPCs showed a positive bias for mean particle diameter and a CV of less than 10%, suggesting acceptable inter-sensor variability for measurements of mean particle diameter. The laser wavelength of the OPC-N3s varied between 600 and 650 nm and appeared to have some effect on inter-sensor variability in the mean diameter. For the number concentration, the OPCs showed a negative bias, compared to the APS, and inter-sensor variability increased with the particle target diameter, i.e., CV of 19.5% for 2 μ m and 34.2% for the 10 μ m target diameter. The flow rate reported by the sensor appeared to affect the inter-sensor variability of the number concentration. The inter-sensor variability (CV of 19.5–47.1%) was higher when using the sensor-reported flow rate, instead of manufacturer-reported constant flow rate of 4.67 mL/s (CV of 5.8–21.7%). Our results suggest that the OPCs are susceptible to inter-sensor variability, which should be considered as part of field deployment, and that the PMS6003 and PMS003 are incapable of correctly sizing particles larger than 2 μ m.

Authors contribution

KK conducted the experiments, and collected, and analyzed the data. KK developed the original draft and KEK reviewed the original

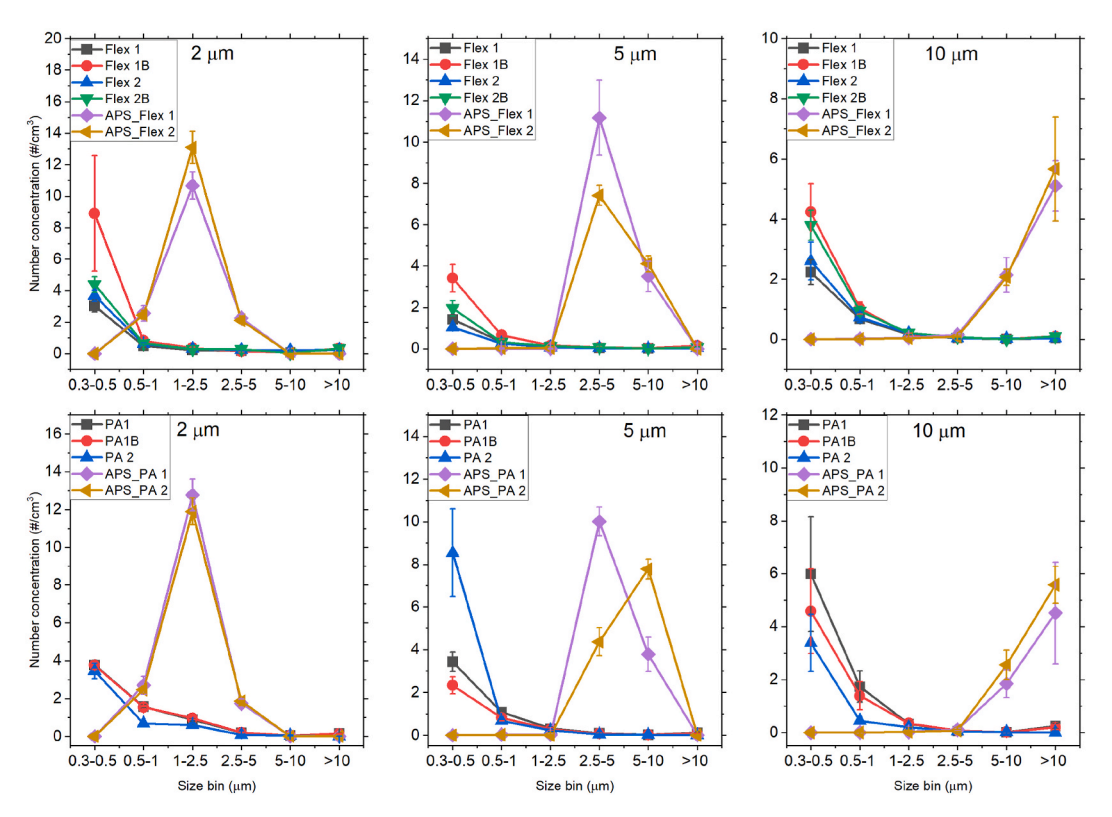


Fig. 8. PSD of Purple Air II Flex (Flex, with PMS6003) and Purple Air II (PA, with PMS5003) vs. the APS. The experiments for PA 2 for a target diameter of 5 μm were performed on a different day than the other sensors. The sensor PA 2B only returned null values. APS_Flex1, APS_Flex2, APS_PA1, and APS_PA2 represent APS measurements taken when conducting evaluation of Flex1, Flex2, PA1, and PA2, respectively. Error bars represent standard deviation (n = 10). APS PSD can be found in the supplementary material, Fig. S11. (For interpretation of the references to colour in this figure legend, the reader is referred to the Web version of this article.)

draft. KEK provided supervision and acquired the funding.

Declaration of competing interest

The authors declare that they have no known competing financial interests or personal relationships that could have appeared to influence the work reported in this paper.

Data availability

Data will be made available on request.

Acknowledgments

This material is based upon work supported by the National Science Foundation under Grant No. 2012091 Collaborative Research Network Cluster: Dust in the Critical Zone and under Grant No. 2228600 CIVIC-PG: TRACK A: Community Resilience through Engaging, Actionable, Timely, High-Resolution Air Quality Information (CREATE-AQI). Thanks to PurpleAir for donating two PAIIs to the project. Thanks to Dr. Eric Pardyjak and Dr. Sebastian Hoch for lending OPCs for this study.

Appendix A. Supplementary data

Supplementary data to this article can be found online at https://doi.org/10.1016/j.jaerosci.2023.106181.

References

- Araújo, I., Costa, D., & de Moraes, R. (2014). Identification and characterization of particulate matter concentrations at construction jobsites. Sustainability, 6(11), 7666–7688. https://doi.org/10.3390/su6117666
- Azarmi, F., Kumar, P., Marsh, D., & Fuller, G. (2016). Assessment of the long-term impacts of PM $_{10}$ and PM $_{2.5}$ particles from construction works on surrounding areas. Environmental Sciences: Processes & Impacts, 18(2), 208–221. https://doi.org/10.1039/C5EM00549C
- Barkjohn, K. K., Gantt, B., & Clements, A. L. (2021). Development and application of a United States-wide correction for PM2.5 data collected with the PurpleAir sensor. Atmospheric Measurement Techniques, 14(6), 4617–4637. https://doi.org/10.5194/AMT-14-4617-2021
- Baron, P., Deye, G. J., Martinez, A. B., Jones, E. N., & Bennett, J. S. (2008). Size shifts in measurements of droplets with the aerodynamic particle sizer and the aerosizer. Aerosol Science and Technology, 42(3), 201–209. https://doi.org/10.1080/02786820801958734
- Bezantakos, S., Schmidt-Ott, F., & Biskos, G. (2018). Performance evaluation of the cost-effective and lightweight Alphasense optical particle counter for use onboard unmanned aerial vehicles. Aerosol Science and Technology, 52(4), 385–392. https://doi.org/10.1080/02786826.2017.1412394
- Bílek, J., Bílek, O., Maršolek, P., & Buček, P. (2021). Ambient air quality measurement with low-cost optical and electrochemical sensors: An evaluation of continuous year-long operation. *Environments MDPI, 8*(11). https://doi.org/10.3390/environments8110114
- Bi, J., Wildani, A., Chang, H. H., & Liu, Y. (2020). Incorporating low-cost sensor measurements into high-resolution PM _{2.5} modeling at a large spatial scale. Environmental Science and Technology, 54(4), 2152–2162. https://doi.org/10.1021/acs.est.9b06046
- Bulot, F. M. J., Russell, H. S., Rezaei, M., Johnson, M. S., Ossont, S. J. J., Morris, A. K. R., Basford, P. J., Easton, N. H. C., Foster, G. L., Loxham, M., & Cox, S. J. (2020). Laboratory comparison of low-cost particulate matter sensors to measure transient events of pollution. Sensors, 20(8), 2219. https://doi.org/10.3390/s20082219
- Cai, M., Zhang, S., Lin, X., Qian, Z., McMillin, S. E., Yang, Y., Zhang, Z., Pan, J., & Lin, H. (2022). Association of ambient particulate matter pollution of different sizes with in-hospital case fatality among stroke patients in China. *Neurology*, 98(24), e2474–e2486. https://doi.org/10.1212/WNL.000000000000200546
- Caplin, A., Ghandehari, M., Lim, C., Glimcher, P., & Thurston, G. (2019). Advancing environmental exposure assessment science to benefit society. *Nature Communications*, 10(1), 1236. https://doi.org/10.1038/s41467-019-09155-4
- Caubel, J. J., Cados, T. E., Preble, C.v., & Kirchstetter, T. W. (2019). A distributed network of 100 black carbon sensors for 100 Days of air quality monitoring in west Oakland, California. *Environmental Science and Technology*, 53(13), 7564–7573. https://doi.org/10.1021/acs.est.9b00282
- Chatzidiakou, L., Krause, A., Han, Y., Chen, W., Yan, L., Popoola, O. A. M., Kellaway, M., Wu, Y., Liu, J., Hu, M., Barratt, B., Cai, Y., Chan, Q., Chatzidiakou, L., Chen, S., Chen, W., Chen, X., Elliott, P., Ezzati, M., ... Jones, R. L. (2020). Using low-cost sensor technologies and advanced computational methods to improve dose estimations in health panel studies: Results of the AIRLESS project. *Journal of Exposure Science and Environmental Epidemiology*, 30(6), 981–989. https://doi.org/10.1038/s41370-020-0259-6, 2020 30:6.
- Chen, B. T., Cheng, Y. S., & Yeh, H. C. (1990). A study of density effect and droplet deformation in the TSI aerodynamic particle sizer. Aerosol Science and Technology, 12(2), 278–285. https://doi.org/10.1080/02786829008959346
- Chojer, H., Branco, P. T. B. S., Martins, F. G., Alvim-Ferraz, M. C. M., & Sousa, S. I. V. (2022). Can data reliability of low-cost sensor devices for indoor air particulate matter monitoring be improved? An approach using machine learning. *Atmospheric Environment*, 286, Article 119251. https://doi.org/10.1016/J.
- Clements, A., Srivastava, M., Conner, T., Rice, J., Habel, A., Reece, S., & Williams, D. R. (2018). Field performance evaluation of four low-cost particulate matter sensors. In Air sensor international conference. https://cfpub.epa.gov/si/si_public_record_report.cfm?Lab=NERL&dirEntryId=342318.
- Consonni, D., Carugno, M., de Matteis, S., Nordio, F., Randi, G., Bazzano, M., Caporaso, N. E., Tucker, M. A., Bertazzi, P. A., Pesatori, A. C., Lubin, J. H., & Landi, M. T. (2018). Outdoor particulate matter (PM10) exposure and lung cancer risk in the EAGLE study. *PLoS One, 13*(9), Article e0203539. https://doi.org/10.1371/
- Crawford, B., Hagan, D. H., Grossman, I., Cole, E., Holland, L., Heald, C. L., & Kroll, J. H. (2021). Mapping pollution exposure and chemistry during an extreme air quality event (the 2018 K-Ilauea eruption) using a low-cost sensor network. *Proceedings of the National Academy of Sciences of the United States of America, 118*(27), Article e2025540118. https://doi.org/10.1073/PNAS.2025540118/SUPPL_FILE/PNAS.2025540118.SAPP.PDF
- Crilley, L. R., Shaw, M., Pound, R., Kramer, L. J., Price, R., Young, S., Lewis, A. C., & Pope, F. D. (2018). Evaluation of a low-cost optical particle counter (Alphasense OPC-N2) for ambient air monitoring. *Atmospheric Measurement Techniques*, 11(2), 709–720. https://doi.org/10.5194/amt-11-709-2018
- Demanega, I., Mujan, I., Singer, B. C., Andelković, A. S., Babich, F., & Licina, D. (2021). Performance assessment of low-cost environmental monitors and single sensors under variable indoor air quality and thermal conditions. *Building and Environment*, 187, Article 107415. https://doi.org/10.1016/j.buildenv.2020.107415
- Do, K., Yu, H., Velasquez, J., Grell-Brisk, M., Smith, H., & Ivey, C. E. (2021). A data-driven approach for characterizing community scale air pollution exposure disparities in inland Southern California. *Journal of Aerosol Science*, 152, Article 105704. https://doi.org/10.1016/J.JAEROSCI.2020.105704
- Duan, H., Romay, F. J., Li, C., Naqwi, A., Deng, W., & Liu, B. Y. H. (2016). Generation of monodisperse aerosols by combining aerodynamic flow-focusing and mechanical perturbation. Aerosol Science and Technology, 50(1), 17–25. https://doi.org/10.1080/02786826.2015.1123213
- Dubey, R., Patra, A. K., Joshi, J., Blankenberg, D., Kolluru, S. S. R., Madhu, B., & Raval, S. (2022). Evaluation of low-cost particulate matter sensors OPC N2 and PM Nova for aerosol monitoring. *Atmospheric Pollution Research*, 13(3), Article 101335. https://doi.org/10.1016/j.apr.2022.101335
- Dubey, R., Patra, A. K., Joshi, J., Blankenberg, D., & Nazneen. (2022). Evaluation of vertical and horizontal distribution of particulate matter near an urban roadway using an unmanned aerial vehicle. The Science of the Total Environment, 836, Article 155600. https://doi.org/10.1016/j.scitotenv.2022.155600
- Duvall, M. R., Clements, L. A., Hagler, G., Kamal, A., Kilaru, V., Goodman, L., Frederick, S., Barkjohn, K. K., VonWal, I., Greene, D., & Tim Dye. (2021). Performance testing protocols, metrics, and target values for fine particulate matter air sensors: Use in ambient, outdoor, fixed site, non-regulatory supplemental and informational monitoring applications. https://cfpub.epa.gov/si/si public record Report.cfm?dirEntryId=350785&Lab=CEMM.
- EPA. (2014). Evaluation of field-deployed low cost PM sensors. www.epa.gov/ord.
- EPA. (2022). EPA interactive map of air quality monitors | US EPA. https://www.epa.gov/outdoor-air-quality-data/interactive-map-air-quality-monitors.
- Giordano, M. R., Malings, C., Pandis, S. N., Presto, A. A., McNeill, V. F., Westervelt, D. M., Beekmann, M., & Subramanian, R. (2021). From low-cost sensors to high-quality data: A summary of challenges and best practices for effectively calibrating low-cost particulate matter mass sensors. *Journal of Aerosol Science*, 158, Article 105833. https://doi.org/10.1016/J.JAEROSCI.2021.105833
- Gomes, J., Esteves, H., & Rente, L. (2022). Influence of an extreme Saharan dust event on the air quality of the west region of Portugal. *Gases*, 2(3), 74–84. https://doi.org/10.3390/gases2030005
- Hagan, D. H., & Kroll, J. H. (2020). Assessing the accuracy of low-cost optical particle sensors using a physics-based approach. Atmospheric Measurement Techniques, 13 (11), 6343–6355, https://doi.org/10.5194/amt-13-6343-2020
- Hegde, S., Min, K. T., Moore, J., Lundrigan, P., Patwari, N., Collingwood, S., Balch, A., & Kelly, K. E. (2020). Indoor household particulate matter measurements using a network of low-cost sensors. *Aerosol and Air Quality Research*, 20(2), 381–394. https://doi.org/10.4209/AAQR.2019.01.0046
- Jacobs, M., Zhang, G., Chen, S., Mullins, B., Bell, M., Jin, L., Guo, Y., Huxley, R., & Pereira, G. (2017). The association between ambient air pollution and selected adverse pregnancy outcomes in China: A systematic review. The Science of the Total Environment, 579, 1179–1192. https://doi.org/10.1016/J. SCITOTENV.2016.11.100
- Japuntich, D. A., Stenhouse, J. I. T., & Liu, B. Y. H. (1990). Conditions for monodispersity of heterogeneous condensation aerosols using dimensionless groups. *Journal of Colloid and Interface Science*, 136(2), 393–400. https://doi.org/10.1016/0021-9797(90)90386-3
- Karagulian, F., Barbiere, M., Kotsev, A., Spinelle, L., Gerboles, M., Lagler, F., Redon, N., Crunaire, S., & Borowiak, A. (2019). Review of the performance of low-cost sensors for air quality monitoring. *Atmosphere*, 10(9), 506. https://doi.org/10.3390/atmos10090506
- Keet, C. A., Keller, J. P., & Peng, R. D. (2018). Long-Term coarse particulate matter exposure is associated with asthma among children in medicaid. *American Journal of Respiratory and Critical Care Medicine*, 197(6), 737–746. https://doi.org/10.1164/rccm.201706-1267OC
- Kelly, K. E., Xing, W. W., Sayahi, T., Mitchell, L., Becnel, T., Gaillardon, P.-E., Meyer, M., & Whitaker, R. T. (2021). Community-based measurements reveal unseen differences during air pollution episodes. *Environmental Science and Technology*, 55(1), 120–128. https://doi.org/10.1021/acs.est.0c02341

- Khreis, H., Johnson, J., Jack, K., Dadashova, B., & Park, E. S. (2022). Evaluating the performance of low-cost air quality monitors in Dallas, Texas. *International Journal of Environmental Research and Public Health*, 19(3), 1647. https://doi.org/10.3390/ijerph19031647
- Kim, K. Y., Kim, Y. S., Roh, Y. M., Lee, C. M., & Kim, C. N. (2008). Spatial distribution of particulate matter (PM10 and PM2.5) in Seoul Metropolitan Subway stations. Journal of Hazardous Materials, 154(1–3), 440–443. https://doi.org/10.1016/j.jhazmat.2007.10.042
- Kosmopoulos, G., Salamalikis, V., Pandis, S. N., Yannopoulos, P., Bloutsos, A. A., & Kazantzidis, A. (2020). Low-cost sensors for measuring airborne particulate matter: Field evaluation and calibration at a South-Eastern European site. Science of the Total Environment, 748. https://doi.org/10.1016/j.scitotenv.2020.141396
- Kuula, J., Mäkelä, T., Aurela, M., Teinilä, K., Varjonen, S., González, Ó., & Timonen, H. (2020). Laboratory evaluation of particle-size selectivity of optical low-cost particulate matter sensors. Atmospheric Measurement Techniques, 13(5), 2413–2423. https://doi.org/10.5194/amt-13-2413-2020
- Lee, S. C., & Chang, M. (2000). Indoor and outdoor air quality investigation at schools in Hong Kong. Chemosphere, 41(1-2), 109-113. https://doi.org/10.1016/
- Liang, Y., Sengupta, D., Campmier, M. J., Lunderberg, D. M., Apte, J. S., & Goldstein, A. H. (2021). Wildfire smoke impacts on indoor air quality assessed using crowdsourced data in California. *Proceedings of the National Academy of Sciences of the United States of America, 118*(36). https://doi.org/10.1073/PNAS.2106478118/-/DCSUPPLEMENTAL
- Li, J., Li, H., Ma, Y., Wang, Y., Abokifa, A. A., Lu, C., & Biswas, P. (2018). Spatiotemporal distribution of indoor particulate matter concentration with a low-cost sensor network. Building and Environment, 127, 138–147. https://doi.org/10.1016/J.BUILDENV.2017.11.001
- Li, J., Mattewal, S. K., Patel, S., & Biswas, P. (2020). Evaluation of nine low-cost-sensor-based particulate matter monitors. *Aerosol and Air Quality Research*, 20(2), 254–270. https://doi.org/10.4209/aaqr.2018.12.0485
- Lim, C. C., Kim, H., Vilcassim, M. J. R., Thurston, G. D., Gordon, T., Chen, L.-C., Lee, K., Heimbinder, M., & Kim, S.-Y. (2019). Mapping urban air quality using mobile sampling with low-cost sensors and machine learning in Seoul, South Korea. *Environment International*, 131, Article 105022. https://doi.org/10.1016/j.envint.2019.105022
- Liu, C., Chen, R., Sera, F., Vicedo-Cabrera, A. M., Guo, Y., Tong, S., Coelho, M. S. Z. S., Saldiva, P. H. N., Lavigne, E., Matus, P., Valdes Ortega, N., Osorio Garcia, S., Pascal, M., Stafoggia, M., Scortichini, M., Hashizume, M., Honda, Y., Hurtado-Díaz, M., Cruz, J., ... Kan, H. (2019). Ambient particulate air pollution and daily mortality in 652 cities. New England Journal of Medicine, 381(8), 705–715. https://doi.org/10.1056/NEJMOA1817364
- Mei, H., Han, P., Wang, Y., Zeng, N., Liu, D., Cai, Q., Deng, Z., Wang, Y., Pan, Y., & Tang, X. (2020). Field evaluation of low-cost particulate matter sensors in Beijing. Sensors (Switzerland), 20(16), 1–17. https://doi.org/10.3390/s20164381
- Mukherjee, A., Stanton, L. G., Graham, A. R., & Roberts, P. T. (2017). Assessing the utility of low-cost particulate matter sensors over a 12-week period in the Cuyama valley of California. Sensors (Switzerland), 17(8). https://doi.org/10.3390/s17081805
- Orellano, P., Reynoso, J., Quaranta, N., Bardach, A., & Ciapponi, A. (2020). Short-term exposure to particulate matter (PM10 and PM2.5), nitrogen dioxide (NO2), and ozone (O3) and all-cause and cause-specific mortality: Systematic review and meta-analysis. *Environment International*, 142. https://doi.org/10.1016/J. ENVINT.2020.105876
- Ouimette, J. R., Malm, W. C., Schichtel, B. A., Sheridan, P. J., Andrews, E., Ogren, J. A., & Arnott, W. P. (2022). Evaluating the PurpleAir monitor as an aerosol light scattering instrument. Atmospheric Measurement Techniques, 15(3), 655–676. https://doi.org/10.5194/amt-15-655-2022
- PlanTower. (2022). PMS6003—Laser PM2.5 sensor-plantower technology. https://www.plantower.com/en/products_33/75.html.
- Purcell, E. M., & Pennypacker, C. R. (1973). Scattering and absorption of light by nonspherical dielectric grains. *The Astrophysical Journal*, 186, 705. https://doi.org/10.1086/152538
- Samad, A., Mimiaga, F. E. M., Laquai, B., & Vogt, U. (2021). Investigating a low-cost dryer designed for low-cost PM sensors measuring ambient air quality. Sensors (Switzerland), 21(3), 1–18. https://doi.org/10.3390/s21030804
- Sayahi, T., Butterfield, A., & Kelly, K. E. (2019). Long-term field evaluation of the Plantower PMS low-cost particulate matter sensors. *Environmental Pollution*, 245, 932–940. https://doi.org/10.1016/j.envpol.2018.11.065
- Singer, B. C., & Delp, W. W. (2018). Response of consumer and research grade indoor air quality monitors to residential sources of fine particles. *Indoor Air*, 28(4), 624–639. https://doi.org/10.1111/JNA.12463
- Singh, S. K., Singh, R. K., Singh, R. K., Singh, R. K., & Singh, S. (2022). Concentration, sources and health effects of silica in ambient respirable dust of Jharia Coalfields Region, India. Environmental Sciences Europe, 34(1), 68. https://doi.org/10.1186/s12302-022-00651-x
- Sousan, S., Koehler, K., Hallett, L., & Peters, T. M. (2016). Evaluation of the Alphasense optical particle counter (OPC-N2) and the Grimm portable aerosol spectrometer (PAS-1.108). Aerosol Science and Technology, 50(12), 1352–1365. https://doi.org/10.1080/02786826.2016.1232859
- Sousan, S., Regmi, S., & Park, Y. M. (2021). Laboratory evaluation of low-cost optical particle counters for environmental and occupational exposures. Sensors, 21(12). https://doi.org/10.3390/s21124146
- Streuber, D., Park, Y. M., & Sousan, S. (2022). Laboratory and field evaluations of the GeoAir2 air quality monitor for use in indoor environments. *Aerosol and Air Quality Research*, 22(8). https://doi.org/10.4209/aaqr.220119
- Technical Specifications OPC-N3 Particle Monitor. (2019). Alphasense Ltd. https://www.alphasense.com/wp-content/uploads/2022/09/Alphasense_OPC-N3_datasheet.pdf.
- Tryner, J., Mehaffy, J., Miller-Lionberg, D., & Volckens, J. (2020). Effects of aerosol type and simulated aging on performance of low-cost PM sensors. *Journal of Aerosol Science*, 150, Article 105654. https://doi.org/10.1016/j.jaerosci.2020.105654
- TSI. (2006). Aerosol instrument manager ® software for aerodynamic particle sizer ® (APS TM) spectrometers user's manual.
- TSI. (2022). Flow-focusing monodisperse aerosol generator. https://tsi.com/getmedia/e90fb381-077a-4106-ab79-eb3ca6078ca7/1520-FMAG_A4_5002133_RevA-WEB? ext=.pdf.
- Vogt, M., Schneider, P., Castell, N., & Hamer, P. (2021). Assessment of low-cost particulate matter sensor systems against optical and gravimetric methods in a field co-location in Norway. Atmosphere, 12(8). https://doi.org/10.3390/atmos12080961
- Volckens, J., & Peters, T. M. (2005). Counting and particle transmission efficiency of the aerodynamic particle sizer. *Journal of Aerosol Science*, 36(12), 1400–1408. https://doi.org/10.1016/J.JAEROSCI.2005.03.009
- WHO. (2021). Ambient (outdoor) air pollution. https://www.who.int/news-room/fact-sheets/detail/ambient-(outdoor)-air-quality-and-health.
- Xiang, H. L., Yang, J., Qiu, Z. Z., Lei, W. X., Zeng, T. T., & Lan, Z. C. (2015). Health risk assessment of tunnel workers based on the investigation and analysis of occupational exposure to PM10. Huan Jing Ke Xue= Huanjing Kexue, 36(8), 2768–2774. https://doi.org/10.13227/j.hjkx.2015.08.006
- Yee, J., Cho, Y. A., Yoo, H. J., Yun, H., & Gwak, H. S. (2021). Short-term exposure to air pollution and hospital admission for pneumonia: A systematic review and meta-analysis. Environmental Health: A Global Access Science Source, 20(1), 6. https://doi.org/10.1186/S12940-020-00687-7
- Zheng, X., Ding, H., Jiang, L., Chen, S., Zheng, J., Qiu, M., Zhou, Y., Chen, Q., & Guan, W. (2015). Association between air pollutants and asthma emergency room visits and hospital admissions in time series studies: A systematic review and meta-analysis. *PLoS One*, 10(9), Article e0138146. https://doi.org/10.1371/journal.pone.0138146